

Benchmarks for Validating Range-Dependent Seismo-Acoustic Propagation Codes

Joo Thiam Goh, *Member, IEEE*, Henrik Schmidt, Peter Gerstoft, and Woojae Seong

Abstract—The availability of fast and relatively low-cost computing power has resulted in radical changes to the role of seismo-acoustic modeling. With the increase in the number of models available, there is the inevitable question of how can one go about validating all these numerical schemes. Recently, the issue of establishing reference solutions for range-dependent ocean acoustic problems was addressed within the Acoustical Society of America. This has resulted in a set of well-defined benchmarks for range-dependent fluid problems. However, to date, there is no consistent set of benchmarks for the range-dependent seismo-acoustic codes. In this paper, we present a collection of problems intended for general use by the modeling community for validation of new computational schemes. A number of new seismo-acoustic codes are applied to produce reference solutions for these benchmarks.

Index Terms—Benchmarking, elastic, modeling.

I. INTRODUCTION

IN OCEAN acoustics, the recent shift in emphasis from deep to shallow water and littoral environments has led to a significant effort in developing environmental acoustics models incorporating improved treatment of the dominant phenomenon in such environments—the bottom interaction.

The shallow-water environment is an extremely complicated waveguide bounded above by a rough sea surface and below by an inhomogeneous, multilayered elastic sea bed. Further, the acoustic properties of the water column are affected by the close proximity to the atmosphere, giving rise to a significant spatial and temporal variability. The elastic sea bed adds another degree of complication and it is only recently that modelers have been able to account for its effect, to some degree. The existence of seismic interface waves, inhomogeneous waves, and headwaves, and interference of multiply reflected waves are all important phenomena, and the energy carried by seismic waves is not negligible compared to the waterborne field.

The most general approaches to modeling seismo-acoustic bottom interaction are the direct numerical solutions to the

Manuscript received June 12, 1996; revised December 17, 1996. This work was supported in part by the Office of Naval Research, in part by the High Latitude Dynamics and the Ocean Acoustics programs.

J. T. Goh is with the Defence Science Organization, Singapore 118230, Republic of Singapore.

H. Schmidt is with the Department of Ocean Engineering, Massachusetts Institute of Technology, Cambridge, MA 02142 USA.

P. Gerstoft is with SACLANT Undersea Research Centre, 19138 La Spezia, Italy.

W. Seong is with the Department of Ocean Engineering, Seoul National University, Seoul 151-742, Korea.

Publisher Item Identifier S 0364-9059(97)03400-6.

elastic and fluid wave equations. Thus, fluid-elastic interaction problems have been handled using both finite-difference methods (FDM's) [1], and finite-element methods (FEM's) [2]. However, since these methods rely on spatial and temporal discretizations which are small compared to the wavelengths, they are normally restricted to modeling short-range propagation and scattering. Even with today's computers, the use of FDM and FEM to problems involving ranges of hundreds or thousands of wavelengths, characteristic of ocean acoustics, is prohibitive.

The *parabolic equation* (PE) algorithm today is without doubt the most popular and versatile approach to modeling range-dependent ocean waveguides. However, in trying to extend the PE theory to elastic medium, two main problems arise. Firstly, the field is described by a vector (displacement) rather than a scalar. Secondly, two different wave speeds exist in a solid and in a heterogeneous media or at boundaries, there is continuous conversion from one wave type to another. Furthermore, elastic bottoms support a wide spectrum of propagation angles. Therefore, even though several PE models have been proposed for wave propagation in elastic media [3]–[9], only a few of these models were actually implemented. Notable implementations include those of Wetton and Brooke [7] and Collins [8], [9]. Thus, for the most part, the parabolic theories for elastic waves have not been adequately tested numerically, particularly in two-way formulations. In addition to being limited to weak range dependence, a major drawback of the PE as well as the discrete methods is the fact that the solutions are not as easily interpreted physically. Thus, the modal structure of the field can only be determined through postprocessing [10].

For range-independent seismo-acoustic propagation modeling, SAFARI [11] is in widespread use for providing exact reference solutions. Since SAFARI is based on integral transforms of the wave equation, it is not directly applicable to range-dependent problems. To overcome this inherent limitation of spectral approaches, Lu and Felsen [12] derived an adiabatic transformation of the wavenumber integrals for weakly range-dependent problems. However, their method works well only for cases where the wave field is largely dominated by *discrete modes* [13]. Its extension to the elastic case is also nontrivial—if at all possible.

Recently, two new modeling approaches were developed for solving the elastic wave equation in range-dependent environments. Both divide the environment into horizontally stratified sectors, coupled along vertical interfaces. Another common feature is the use of wavenumber integration for

generating the Green's functions for the sectors. The main difference is the handling of the coupling of seismic energy at the vertical interfaces between these range-independent sectors. One, in principle, exact method—the so-called *spectral super-element* approach—solves the coupled integral equation using a high-order panel-boundary-element formulation [14], [15]. The other approximate approach solves the reflection/transmission problem locally at a discrete number of depths, yielding a distribution of virtual panel sources [16]. Both methods use standard wavenumber integration to compute the forward and backward scattered field within the sectors. The testing and validation of these new codes as well as the elastic PE has been hampered by the lack of benchmarks with associated reference solutions as well as the availability of other general-purpose seismo-acoustic propagation codes.

This paper presents a series of canonical benchmark problems, providing the elastic equivalents of the ASA benchmarks now used extensively as a standard by the modeling community [17]. The benchmark problems presented here are a subset of the very extensive list of benchmark problems used by the authors in recent years for validating new seismo-acoustic models [18]. These benchmarks also include elastic versions of problems solved in a recent workshop on reverberation and scattering [19].

Each individual benchmark problem presented here has been selected to emphasize a specific critical issue. Thus, for example, one of the problems emphasizes robustness of the backscatter solutions for low-contrast, lateral discontinuities. As the other extreme, another problem tests the accuracy of the various models in handling strong compression/shear coupling at elastic interfaces.

Some of the modeling approaches have extreme difficulty handling one class of problems, but performed very well for others. In addition, there is no unique yardstick for modeling performance. Thus, for some applications, accuracy is crucial, while for others, computational efficiency is the dominant requirement. Consequently, this paper does not attempt in any way to objectively compare code performance. In other words, the results are not the outcome of a “shoot-out” among the various codes. The objective of this paper is solely to present a series of benchmark problems to which future new modeling approaches may be applied for validation and verification.

II. THE NUMERICAL CODES

Several different numerical codes have been applied to the benchmark problems. On the other hand, this is not to be considered a competition among all existing seismo-acoustic codes, and the list is far from complete.

Our solutions were obtained with the finite-element parabolic equation code by Collins [9], boundary element code by Gerstoft and Schmidt [20], the virtual source algorithm by Schmidt [16], and the spectral super-element code by Goh and Schmidt [15]. The latter three codes use SAFARI as the Green's function generator but handles the coupling at the vertical interfaces in a fundamentally different manner.

The detailed description of the various codes are given elsewhere, but for completeness we here briefly outline the

main features characterizing the codes and their fundamental strengths and limitations.

A. FEPES—Finite Element PE

FEPES is an elastic PE code for time harmonic sound propagation in an ocean overlying a sediment that supports both compressional and shear waves. It incorporates the split-step Padé solution as well as a self starter which properly excites interface waves [8]. FEPES handles all elastic wave types including interface waves and, for range-*independent* problems, it is both arbitrarily accurate and unconditionally stable. FEPES contains an energy-conservation correction which helps improve the accuracy of the PE method for range-*dependent* problems. In FEPES, a range-dependent ocean environment is approximated by a sequence of range-independent regions. The range-independent elastic PE is used to propagate the solution through these range-independent sectors. An amplitude correction, based on energy-flux conservation, is then applied at the vertical interfaces separating each range-independent region, thereby obtaining an approximation to the field transmitted across the vertical interface. Even though the elastic PE is efficient, it is accurate only for gradual range dependence. In particular, it may break down if the range variation in the elastic properties is large, i.e., in problems involving large contrasts across the vertical interfaces. The FEPES code was only used for solving test problem D1.

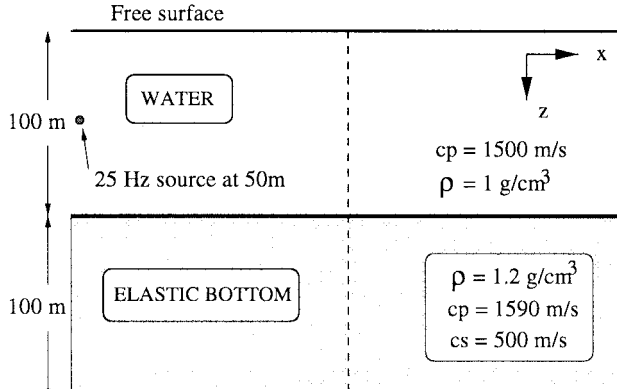
B. BEM—Boundary Element Model

The boundary element method (BEM) of Gerstoft and Schmidt [20] treats propagation and scattering in an environment with two coupled, stratified regions, separated by an arbitrarily shaped contour. The contour is divided into a number of discrete boundary elements with assumed linear field variability. With both coupled regions assumed plane-stratified, the Green's functions are computed by wavenumber integration using SAFARI. This eliminates all boundary integral contributions from the interfaces in the stratification, leaving only the finite region contour in the boundary integral representation. Once the boundary element equations are solved, the scattered field is computed using SAFARI Green's functions again. The BEM code was developed for problems concerning scattering from elastic objects in a stratified seabed and discrete ice cover features such as keels and ridges. However, the general contour shapes allowed make this approach applicable to canonical range-dependent propagation problems involving a single, discrete feature, such as a discrete change in bathymetry or medium characteristics. The BEM code has been thoroughly validated, and for problems where the solutions differ, we expect the BEM solution to be the most accurate.

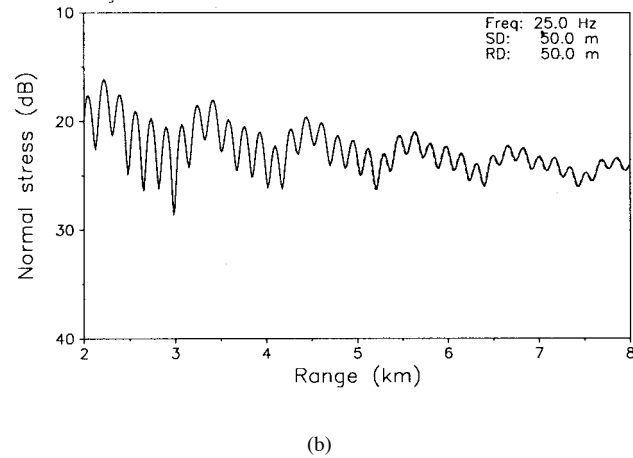
Allowing only linear field variation over the elements, at least ten boundary elements per wavelength are required to ensure convergence of the BEM solutions.

C. CORE—Spectral Super-Element Model

CORE is an acronym for coupled OASES for range-dependent environments [15]. It belongs to the new spectral



(a)



(b)

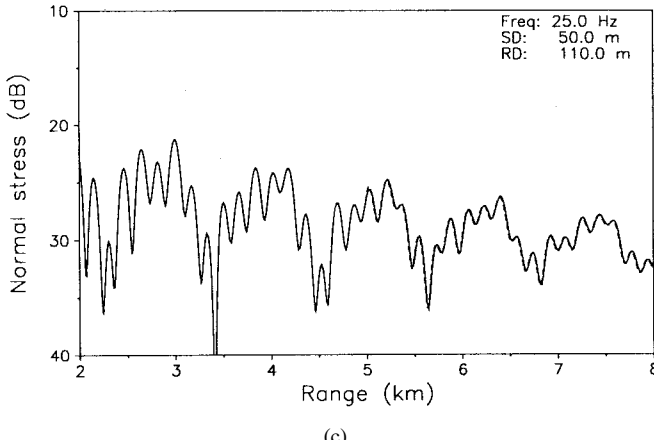


Fig. 1. Modified NORDA 3A test case (ex. A1). (a) Test configuration, (b) receiver at 50 m, and (c) receiver at 110 m. Solid: SAFARI; dashed: CORE.

super-element [14] class of propagation models for range-dependent waveguides. The spectral super-element approach is a hybridization of the finite-element and boundary element methods. The environment is divided into a series of range-independent sectors, separated by vertical interfaces along which the field parameters are expanded in a series of orthogonal polynomials within each layer. The field within the super-element and the influence functions connecting the expansion functions are given by wavenumber integral

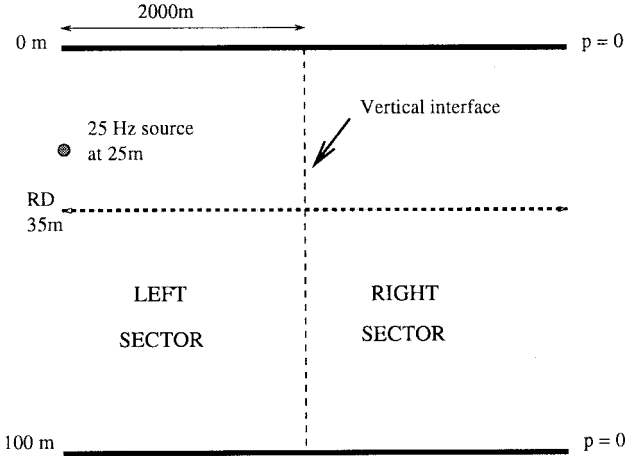


Fig. 2. Example B configuration for single-layer benchmarks.

TABLE I
PARAMETERS FOR THE SERIES OF TWO-SECTOR CANONICAL TEST PROBLEMS

		BENCHMARK			
Parameters		B1	B2	B3	B4
Left sector	ρ	1.0	1.5	1.5	1.5
	c_p	1500	1700	1700	1700
	c_s	0	700	700	700
	α_p	0.2	0.2	0.2	0.2
	α_s	0	0.5	0.5	0.5
Right sector	ρ	1.5	1.0	1.5	1.5
	c_p	1700	1500	1800	3000
	c_s	700	0	900	1700
	α_p	0.2	0.2	0.2	0.2
	α_s	0.5	0	0.5	0.5

Wave speeds are given in m/s, densities in g/cm³, and attenuation in dB/λ.

representations. Thus, the boundary conditions to be satisfied on the vertical interfaces can be expressed in a linear system of equations in the expansion coefficients, with the coefficient matrix evaluated using SAFARI/OASES. The system of equation yields the two-way field in all elements simultaneously, but in most cases a more efficient marching, single-scatter solution can be applied.

All CORE solutions provided here use the single-scatter approximation. Also, unless otherwise noted, the spectral super-element solutions are obtained using only four orders of expansion in the field parameters within each layer.

D. VISA—Virtual Source Approach

The virtual source algorithm (VISA) [16] is similar to the spectral super-element models in terms of the division of the range-dependent waveguide into horizontally stratified sectors. However, instead of the boundary integral solution used to match the boundary conditions in BEM and CORE, VISA uses a marching, local single-scatter approximation to the transmission and reflection problem at the sector boundaries.

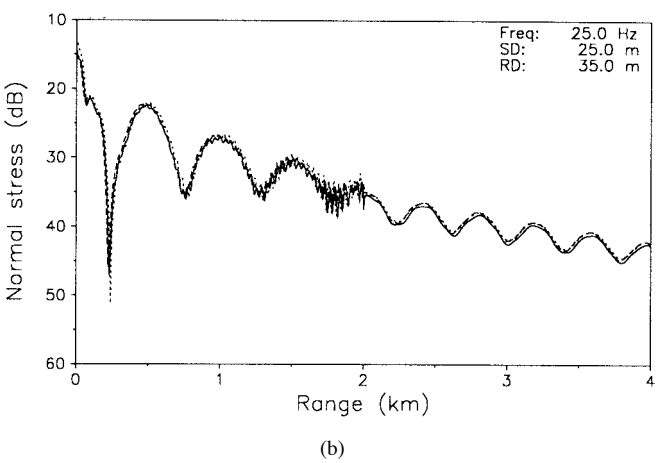
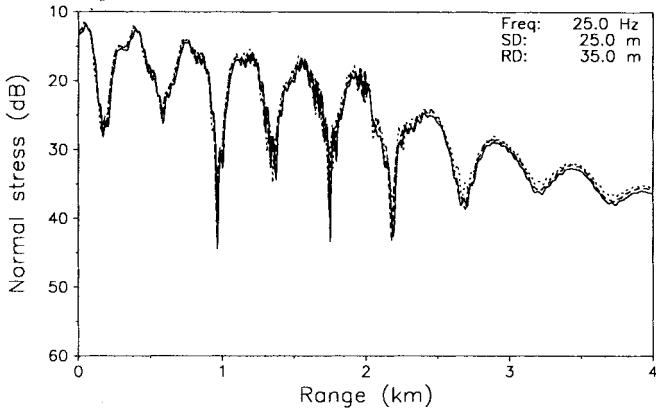


Fig. 3. Solutions to the single-layer benchmarks. (a) Case B1 and (b) Case B2. Solid: BEM; dashed: VISA; dotted: CORE.

Thus, a virtual array of sources and receivers is introduced on each sector boundary. The field incident from the physical source or the previous sector boundary is computed using SAFARI/OASES and therefore inherently decomposed in plane waves. Each plane wave component is then undergoing a local reflection/transmission process, leading to a direct wavenumber integral representation for the displacements on the boundaries. These then act as sources in the virtual source array radiating into the next sector and back into the previous ones. Because it does not depend on the solution of an integral equation, VISA is extremely efficient compared to BEM and CORE, but it obviously provides an approximation only. On the other hand, as the benchmark problems demonstrate, it is extraordinarily robust.

III. ELASTIC BENCHMARK CLASSIFICATION

The benchmark problems we propose can be categorized into several classes and subclasses as follows.

A. Sanity Checks

This class of benchmarks are in general extremely simple problems which are trivial to solve by existing codes. Typical examples are range-independent problems which can be solved exactly using wavenumber integration, but which are nontrivial

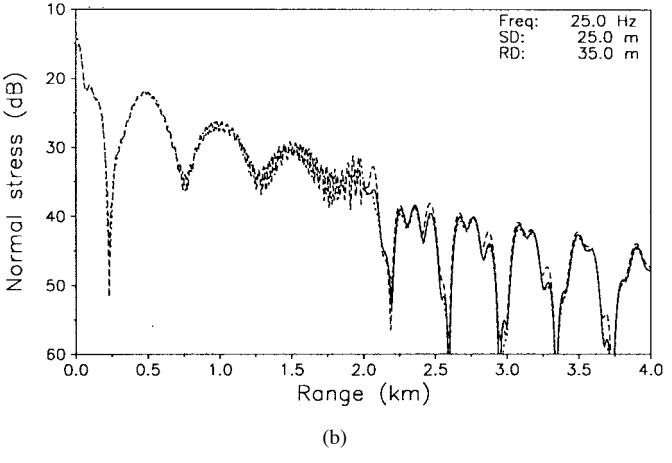
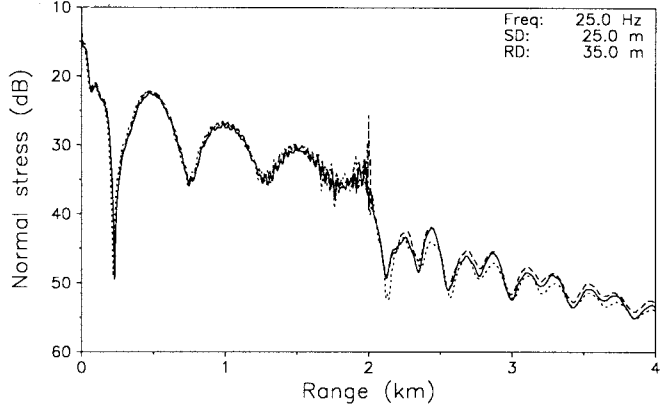
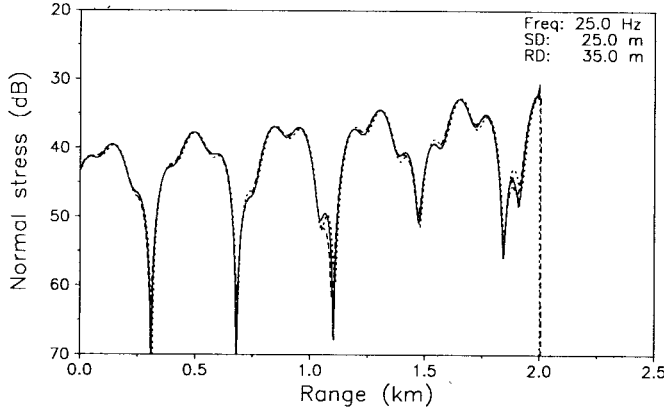


Fig. 4. Solutions to the single-layer benchmarks. (a) Case B3 and (b) case B4. Solid: BEM; dashed: VISA; dotted: CORE.

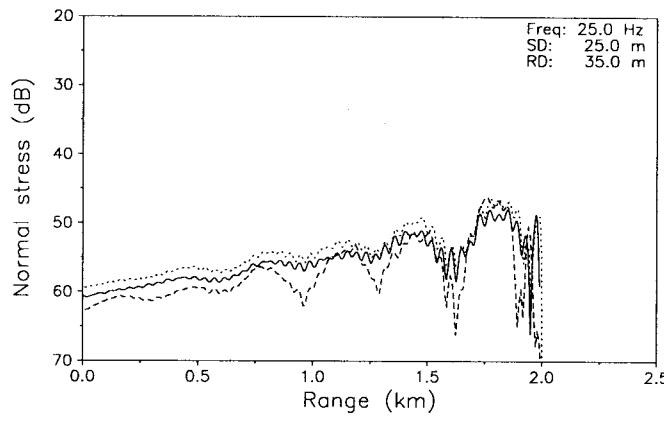
for codes such as CORE and VISA, which handle dummy interfaces in the same manner whether they are transparent or not. These problems are excellent for identifying implementation errors and for testing energy conservation of a marching solution such as the PE or VISA. Also, in the case of elastic problems, improper handling of compression/shear coupling is in general emphasized by these noncoupling problems.

B. Discrete Medium Changes

This class provides the next level of complexity and introduces backscattering. A characteristic example of this class is two welded elastic slabs with only the medium properties changing in the lateral direction. The geometry of the problem remains unchanged in the lateral direction. Depending on the contrast, these problems can be conveniently subdivided into weak and strong subclasses. Weak contrast problems are characterized by small changes in the elastic constants between sectors, typically 10%–20%. Such cases also exhibit weak compression/shear coupling, and models such as most PE's depending on this will work excellently. Some range-dependent problems encountered in the real seabed are characterized by strong contrasts. Since the importance of shear in ocean acoustics is inherently associated with strong coupling, most problems where shear is important are of this category. For horizontal interfaces, strong contrast is handled



(a)



(b)

Fig. 5. Backscatter solutions to the single-layer benchmarks. (a) Case B1 and (b) case B2. Solid: BEM; dashed: VISA; dotted: Core.

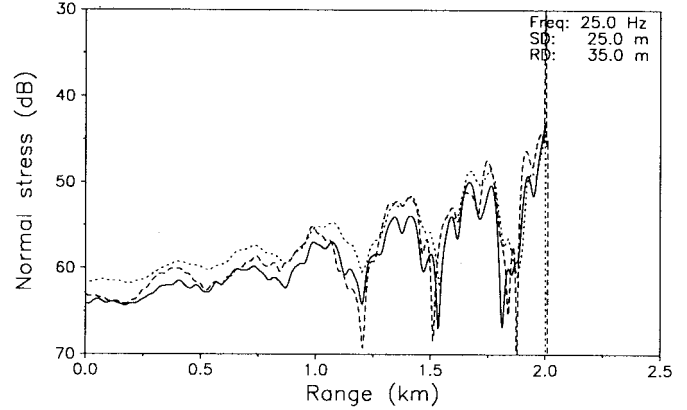
easily by both wavenumber-integration approaches and the PE, but strong contrasts at vertical interfaces provide a serious problem for the PE, for example. Later we introduce a couple of benchmarks which emphasize proper handling of such strong compression/shear coupling.

C. Discrete Geometry Changes

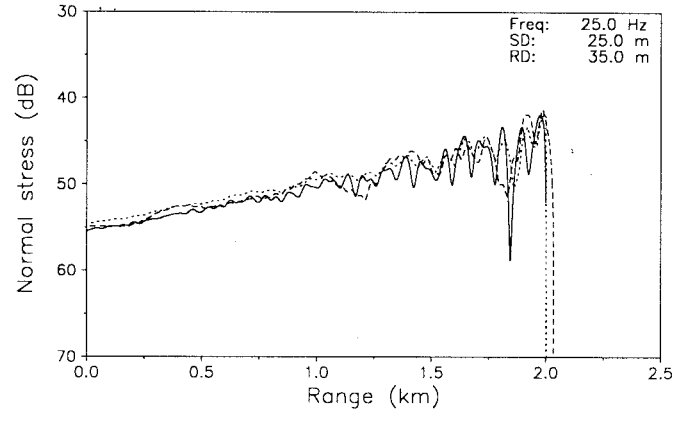
In addition to changes in medium properties, benchmarks in this class also exhibit discrete changes in geometry in the lateral direction. These discrete changes often take the forms of step changes in bathymetry. An example would be the ocean waveguide with a stair-step discontinuity.

D. Continuous Range Variation

This next level of benchmark complexity introduces more realistic gradual range dependence, with the classical example being the ideal and penetrable fluid wedge problems. For computational reasons, these problems are the ones for which the PE is the natural choice of approach. However, for elastic bottoms where compression/shear coupling becomes important, the performance of the elastic PE is uncertain. It may work excellently for small slopes and/or weak contrasts, but the limitations are unknown because of the lack of benchmarks and reference solutions. The establishment of these limitations



(a)



(b)

Fig. 6. Backscatter solutions to the single-layer benchmarks. (a) Case B3 and (b) case B4. Solid: BEM; dashed: VISA; dotted: CORE.

is one of the major issues which can be addressed through benchmarking with some of the new solution techniques.

E. Consistency Benchmarks

This class is very similar to the class described in Section III-A in the sense that they provide a form of sanity check. They do so, however, at a much higher level of complexity, allowing for validation of some of the more subtle issues of fluid–elastic interaction. In general, these problems possess some form of symmetry which make the solutions “self-checking” by virtue of the associated field symmetry properties. A characteristic example of this class is a plane wave or beam incident along the symmetry plane of a corner reflector/refractor. Below we present an example of such a “corner” problem.

IV. BENCHMARK PROBLEMS AND SOLUTIONS

In the following, we present the various benchmarks and the solutions obtained using the various codes described above. In all cases involving a water medium, it is assumed to be lossless with a sound speed of 1500 m/s and a density of 1 g/cm³. The reference level for the solutions is the pressure at 1 m for the point source in free space.

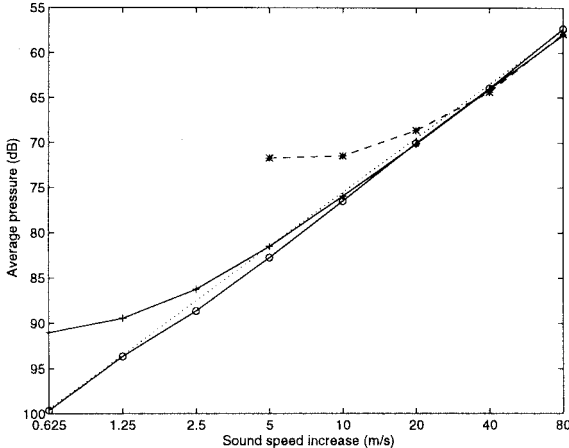


Fig. 7. Dynamic range test. The average field at range zero as a function of sound speed contrast (log scale). *: BEM; +: CORE; ○: VISA. For reference, the dotted line shows a 6-dB increase per sound-speed doubling but with arbitrary absolute location.

A. Sanity Benchmarks

1) A1: Modified NORDA Case 3: Example A1 is based on case 3A used in the NORDA Parabolic Equation Workshop [21]. This problem was first modified for use as a test case for elastic PE by Wetton and Brooke [7] and we run a slightly different version here. The waveguide, illustrated in Fig. 1(a), consists of a water layer with a thickness of 100 m, over a solid layer with a thickness of 100 m, a density of 1.2 g/cm^3 , a compressional speed of 1590 m/s, and a shear speed of 500 m/s. The fluid is assumed to be lossless and the solid has a compressional attenuation of $0.2\text{dB}/\lambda$ and a shear attenuation of $0.5 \text{ dB}/\lambda$. A 25-Hz line source is placed at a distance of 5 km from an artificial transparent interface. The primary test here is to see how well energy is coupled through a transparent vertical interface and represents the extreme case of a low-contrast vertical step. Comparisons between SAFARI and our solutions for receiver depths of 50 and 110 m are shown in Fig. 1(b) and (c). For clarity, we have shown the solution from 2 to 8 km and we see that the super-element solution agrees well with SAFARI. For ranges less than 5 km, the super-element formulation reduces to SAFARI exactly and we see perfect agreement in the solutions. For ranges beyond the artificial interface, the agreement is still quite good for both receivers, indicating proper coupling across the interface.

B. Discrete Medium Changes Benchmarks

1) B1–B4: Single-Layer Benchmarks: The next benchmark consists of a set of two-sector problems shown in Fig. 2. The waveguide is bounded at the top and bottom by a pressure release boundary. A 25-Hz line source is placed at a depth of 25 m and at a distance of 2 km from the vertical discontinuity. By bounding the waveguide by pressure release boundaries, this benchmark requires the propagation code to properly conserve energy before one can arrive at the correct answer. In addition, by varying the material properties on both sides of the discontinuity, we can assess the sensitivity of a particular code to contrast in the primary direction of propagation. Table I shows the four different configurations that we have chosen.

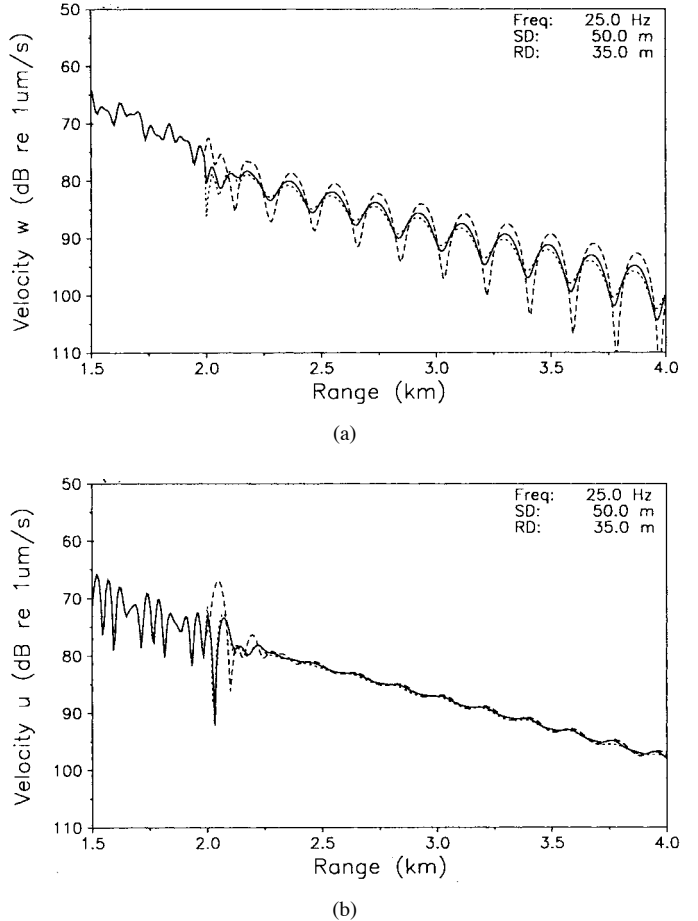
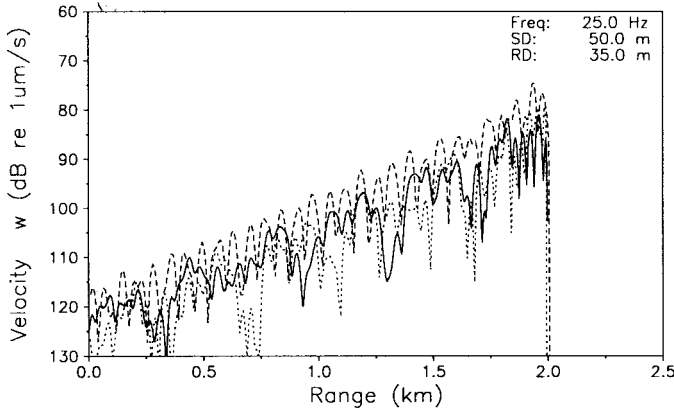


Fig. 8. B6: Mode conversion with a vertical line force. Forward scattered field: (a) vertical particle velocity and (b) horizontal particle velocity. Solid: BEM; dashed: VISA; dotted: CORE.

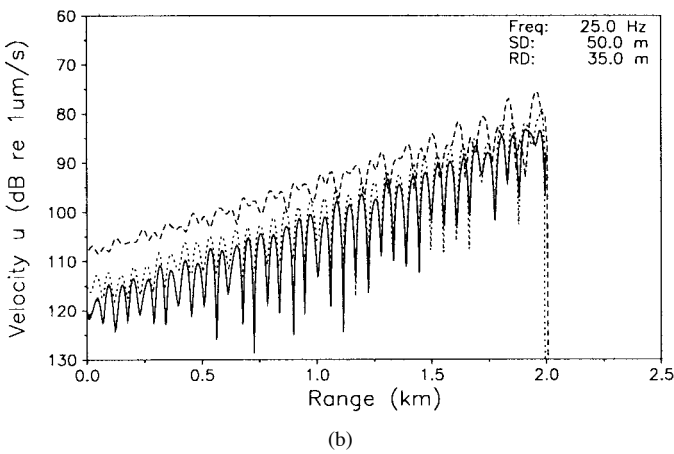
Solutions for the normal stress at a receiver depth of 35 m are shown in Figs. 3 and 4, and we generally have good agreement among the three forward solutions. The backscatter solutions are presented in Figs. 5 and 6. We believe that the differences in the backscatter solutions are due to the large dynamic range in both the forward and backscattered solutions.

2) B5: Dynamic Range Test: For a low-contrast problem, we investigate the dynamic range of each code. For a vertical interface with a low contrast, most energy will penetrate the interface and only little energy will be backscattered. The difference in the fields for which the solution breaks down is referred to as the dynamic range of the codes. The CORE and BEM codes will have greater difficulties in handling such a problem than VISA since they solve for a virtual source distribution on the interface to be used for both the forward and backward field. In doing so, most of the numerical effort will be on obtaining a correct forward field. On the other hand, VISA solves it solely as a transmission and reflection problem and should not experience problems with low contrasts. This test is only for establishing the dynamic range for the codes.

A simple two-sector acoustic case is selected and the average backscattered field in the water column at range zero from a vertical interface at 2-km range is computed. A 25-Hz line source is placed at a depth of 25 m. The



(a)



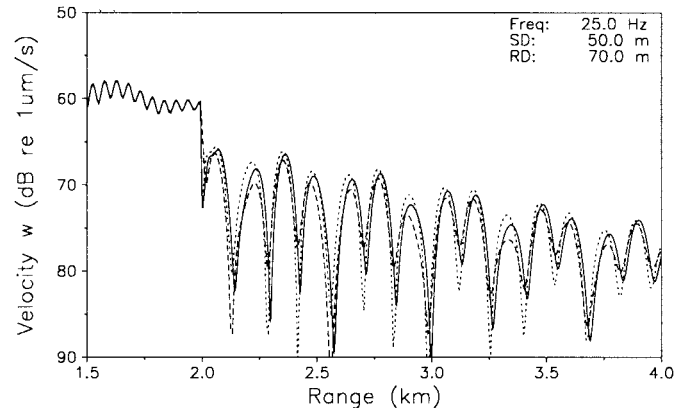
(b)

Fig. 9. B6: Mode conversion with a vertical line force. Backward scattered field: (a) vertical particle velocity and (b) horizontal particle velocity. Solid: BEM; dashed: VISA; dotted: CORE.

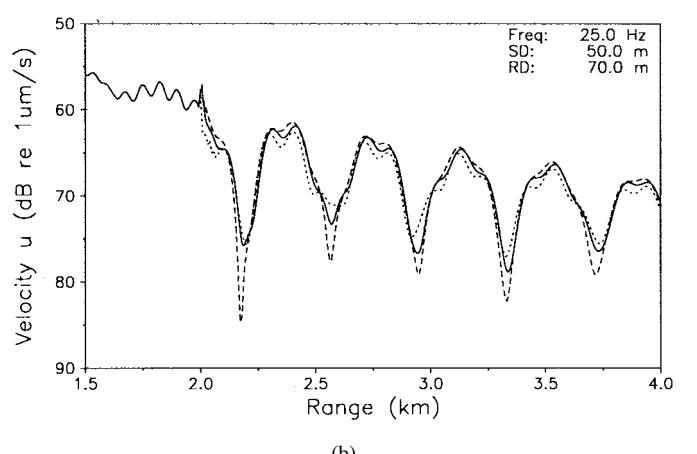
left sector has a nominal sound speed of 1500 m/s and we systematically double the sound-speed difference between the left and right sector from 0.625 to 80 m/s. We will assume that the increment is small and that the arrivals are approximately perpendicular to the interface such that the reflection coefficient doubles for every doubling of the sound-speed differential. This corresponds to a 6-dB increase in the backscattered field. The result of this test, Fig. 7, does in fact show that VISA follows closely the 6-dB increase per sound-speed doubling, while CORE and BEM break down earlier.

Transforming the backscattered field to the vertical interface, the dynamic range, i.e., the difference between the average forward and backward field before the solution breaks down, can be estimated. For BEM, it is about 40 dB and for CORE 55 dB. The larger dynamic range for CORE is expected to be due to its higher order representation of the field at the interface. For more complicated problems involving shear and more complicated geometry, the dynamic range is expected to be lower.

3) B6: Mode Conversion—Vertical Line Force: Mode conversion from compressional waves to shear and vice versa is an extremely important physical process. It is also the single most important complicating factor in most parabolic equation formulations. Example B6 considers just this particular problem.



(a)

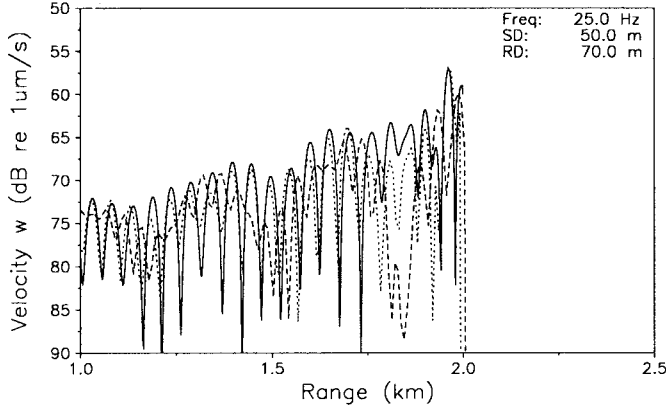


(b)

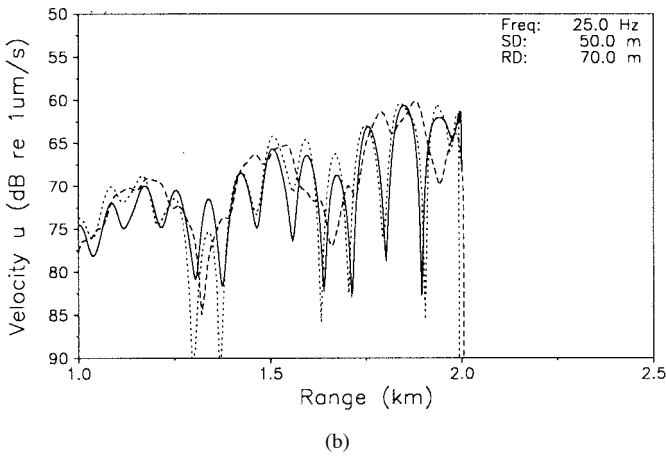
Fig. 10. B7: Mode conversion with a horizontal line force. Forward scattered field: (a) vertical particle velocity and (b) horizontal particle velocity. Solid: BEM; dashed: VISA; dotted: CORE.

A 25-Hz vertical line force of 1 N/m is placed at 50-m depth in a 100-m deep waveguide bounded at the top and bottom by pressure-release boundaries. We set up a two-sector problem with the compressional and shear speed in the left sector being 1700 and 700 m/s, respectively. The density is 1.5 g/cm³ and the compressional and shear attenuation is 0.2 and 0.5 dB/λ, respectively. The right sector is elastic with a compressional speed of 3000 m/s and a shear speed of 1700 m/s. All other parameters remain the same. The compressional speed in the left sector is matched to the shear speed on the right, resulting in strong coupling of *P* waves from the left to *S* waves on the right. Another complicating factor is the extremely large contrast in the sound speeds. The solutions for this example are shown in Figs. 8 and 9. There is generally good agreement between the BEM and CORE solutions in the forward and backscattered directions. The VISA solution differs near the vertical boundary and in the backscattered direction. This is because the VISA approach does not solve the full integral equation at the vertical interface and hence does not permit coupling between the horizontal and vertical displacements at the vertical interface.

4) B7: Mode Conversion—Horizontal Line Force: In Example B7, we run the same problem but this time with a horizontal line force of 1 N/m placed in the middle of the waveguide.

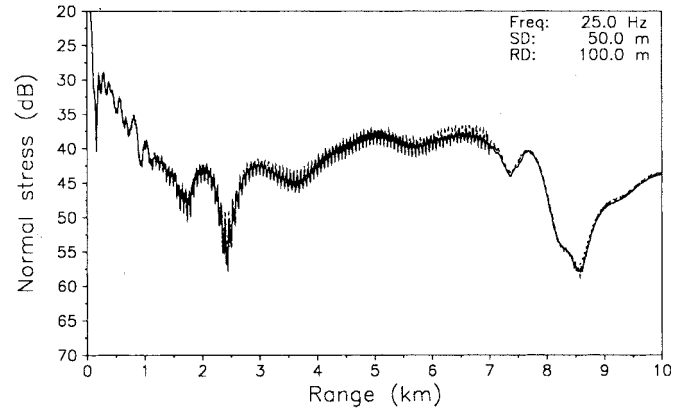


(a)

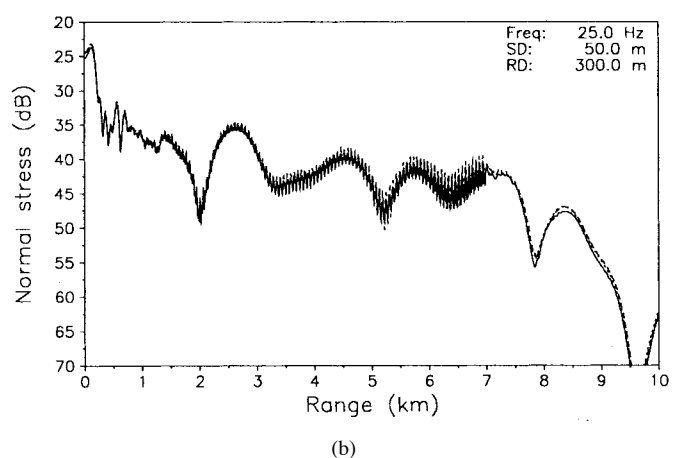


(b)

Fig. 11. B7: Mode conversion with a horizontal line force. Backward scattered field: (a) vertical particle velocity and (b) horizontal particle velocity. Solid: BEM; dashed: VISA; dotted: CORE.



(a)



(b)

Fig. 13. Embedded elastic step (Example C1). Total normal stress. Receiver at (a) 100 m and (b) 300 m. Solid: BEM; dashed: VISA; dotted: CORE.

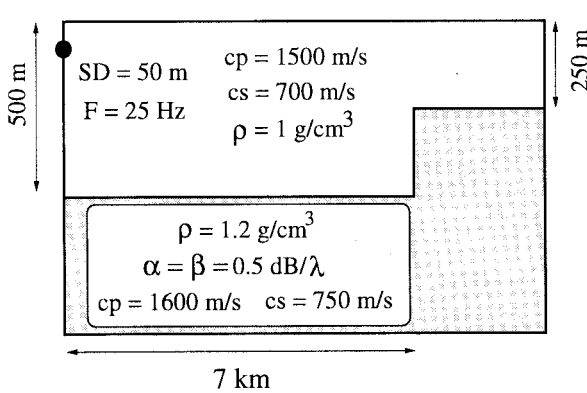


Fig. 12. C1: embedded step discontinuity.

From the symmetry of the waveguide, we can see that now most of the excitation at the vertical discontinuity will be of the compressional waves. The solutions for this example are shown in Figs. 10 and 11.

C. Discrete Geometry Changes Benchmarks

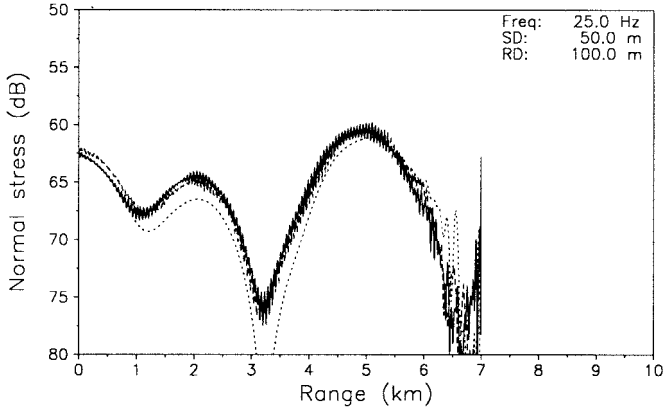
1) C1: Low-Contrast Embedded Elastic Step: Example C1, taken from Collins [8] and shown in Fig. 12, involves two solid layers and a step discontinuity in layer thickness. A 25-Hz line source is placed at a depth of 50 m in the upper layer, which is 500 m thick for ranges less than 7 km and

250 m for ranges beyond 7 km. The compressional and shear speeds in the upper layer is 1500 and 700 m/s, respectively, and the medium is assumed to be lossless. The lower layer is a half-space with compressional and shear speeds equal to 1600 and 750 m/s, respectively. The attenuation in the lower medium is $0.5 \text{ dB}/\lambda$ for both wave types. The density in the upper and lower medium is 1 and $1.2 \text{ g}/\text{cm}^3$, respectively. This particular problem has a very low contrast across the vertical interface and we present forward and backscatter solutions at two receiver depths (Figs. 13 and 14, respectively). In the forward direction, we have good agreement between the three solutions.

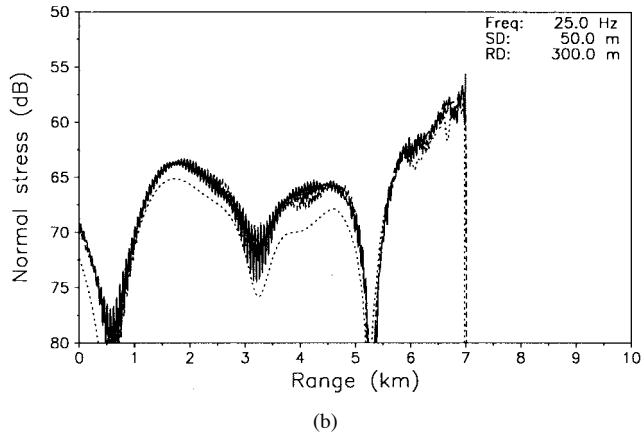
In the backscatter, there is some disagreement, particularly near the scattering surface. We believe this is due to inaccuracies associated with the large dynamic range between the forward and backscattered field.

D. Continuous Range-Variation

1) D1: Elastic ASA Wedge: Example D1, shown in Fig. 15, is test case 3 from the Parabolic Equation Workshop II [22]. This is an elastic version of the standard ASA wedge benchmark problem. A 25-Hz point source is placed at 100 m depth. The ocean depth decreases linearly with range from 200 m at the source range to zero at $r = 4 \text{ km}$. The ocean bottom has a compressional sound speed of 1700 m/s and a shear speed of 800 m/s. The density is $1.5 \text{ g}/\text{cm}^3$ with the



(a)



(b)

Fig. 14. Embedded elastic step (example C1). Backscattered normal stress solution. Receiver at (a) 100 m and (b) 300 m. Solid: BEM; dashed: VISA; dotted: CORE.

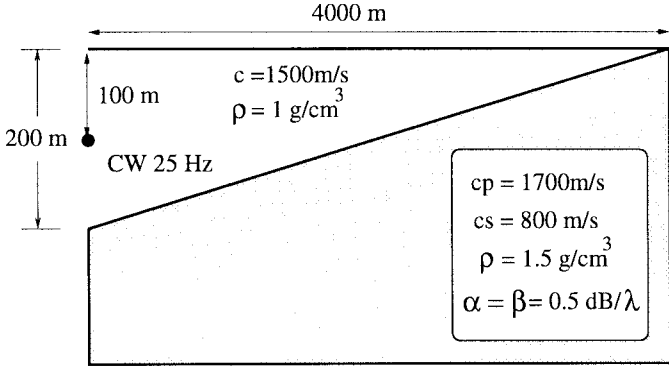
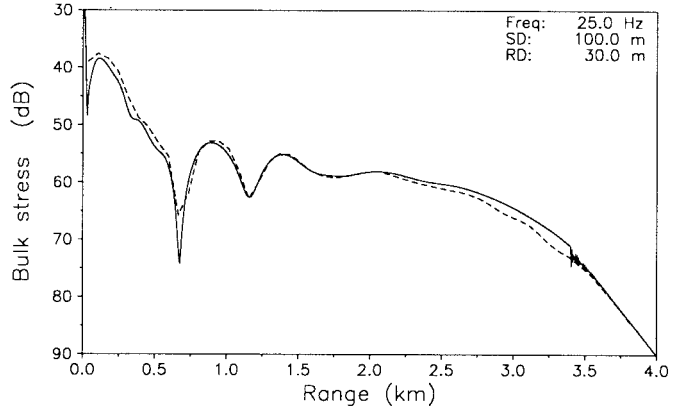


Fig. 15. Environment for the ASA elastic wedge.

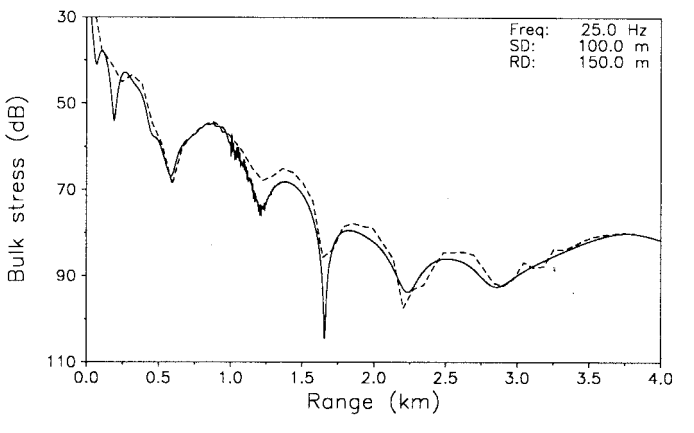
compressional and shear attenuations at $0.5 \text{ dB}/\lambda$. In Fig. 16, we present solutions from the PE model and the super-element method. There is good agreement for the shallow receiver and, for the receiver in the bottom, the agreement is still quite good and the differences are primarily due to the particular manner in which the environment is being discretized.

E. Consistency Benchmarks

1) E1: Corner Reflection/Refraction: Example E1 considers reflection and diffraction from a corner. We have a beam impinging onto a corner of a square at an angle of 45°



(a)



(b)

Fig. 16. ASA elastic wedge (Example D1). Receiver at (a) 30 m and (b) 150 m. Solid: FEPES; dashed: CORE.

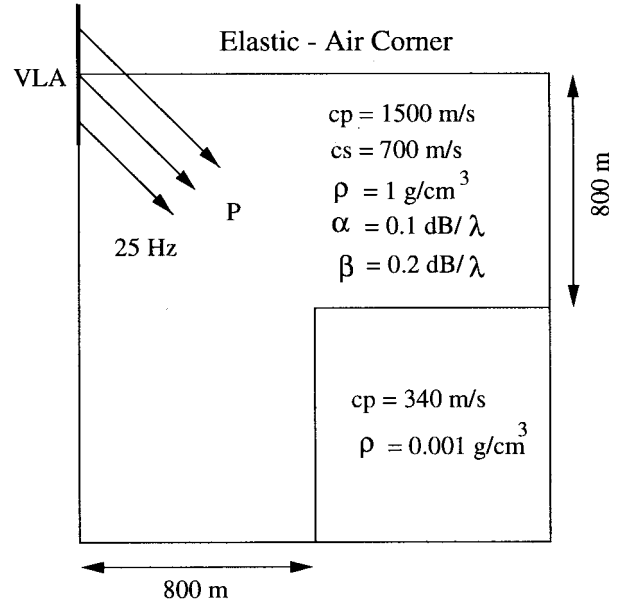


Fig. 17. E1: schematic for elastic-air corner problem.

measured from the horizontal. The array is made up of 20 sources spaced 30 m apart, with Hanning weights applied and extending from the surface down to a depth of 570 m.

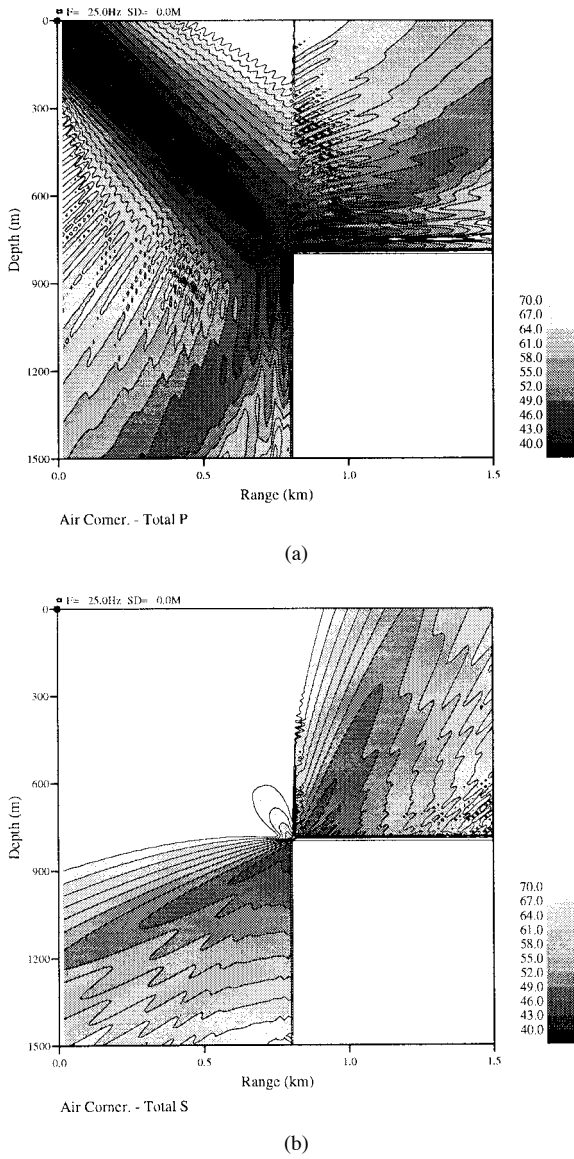


Fig. 18. E1: elastic-air corner—VISA solution: (a) total dilatation and (b) total shear.

Again, we can construct a multitude of different combinations for the host medium (containing the source) as well as the corner. Example E1, shown in Fig. 17, considers the case of an elastic host medium and an air corner. We present only VISA-generated solutions for the total dilatational and shear stress. This test is particularly attractive because of the characteristic symmetric “butterfly” field contour (Fig. 18).

V. CONCLUSION

We have presented solutions to some range-dependent seismo-acoustic problems chosen as benchmarks for validating general-purpose codes. Even though some of these problems do not represent realistic ocean environments, they nevertheless serve the very important objective of testing the integrity of the code as well as the robustness of the formulation. Only when we are confident that the code

behaves as it should can we then apply them to solve “real-world” problems. No doubt many other variations can be derived from the simple examples here. In this paper, we have not provided detailed computational times. Clearly, the more complete solutions provided by BEM and CORE are obtained at an increase in computational cost compared to the approximate solutions provided by VISA and FEPES. A complete set of the solutions can be obtained from the URL <ftp://keel.mit.edu/pub/benchmarks>.

REFERENCES

- [1] R. A. Stephen, “A review of finite-difference methods for seismo-acoustic problems at the sea floor,” *Rev. Geophys.*, vol. 26, pp. 445–458, 1988.
- [2] J. E. Murphy and S. A. Chin-Bing, “A seismo-acoustic finite element model for underwater acoustic propagation,” in *Shear Waves in Marine Sediments*, J. M. Hovem, M. D. Richardson, and R. D. Stoll, Eds., Norwell, MA: Kluwer, 1991.
- [3] J. A. Hudson, “A parabolic approximation for elastic waves,” *Wave Motion*, vol. 2, pp. 207–214, 1980.
- [4] J. P. Coronas, B. DeFacio, and R. J. Krueger, “Parabolic approximations to the time-independent elastic wave equation,” *J. Math. Phys.*, vol. 23, no. 4, pp. 577–586, 1982.
- [5] S. C. Wales and J. J. McCoy, “A comparison of parabolic wave theories for linearly elastic solids,” *Wave Motion*, vol. 5, pp. 99–113, 1983.
- [6] R. R. Greene, “A high-angle one-way wave equation for seismic wave propagation along rough and sloping interfaces,” *J. Acoust. Soc. Amer.*, vol. 77, pp. 1991–1998, 1985.
- [7] B. T. R. Wetton and G. H. Brooke, “One-way wave equations for seismoacoustic propagation in elastic waveguides,” *J. Acoust. Soc. Amer.*, vol. 87, no. 2, pp. 624–632, 1990.
- [8] M. D. Collins, “A two-way parabolic equation method for elastic media,” *J. Acoust. Soc. Amer.*, vol. 93, pp. 1815–1825, 1993.
- [9] ———, “An energy conserving parabolic equation for elastic media,” *J. Acoust. Soc. Amer.*, vol. 94, no. 3, pp. 975–982, 1993.
- [10] F. B. Jensen and H. Schmidt, “Spectral decomposition of PE fields in a wedge-shaped ocean,” in *Progress in Underwater Acoustics*, H. M. Merklinger, Ed., New York: Plenum, 1987.
- [11] H. Schmidt, “SAFARI: Seismo-acoustic fast field algorithm for range independent environments,” User’s guide, SR 113, SACLANT ASW Research Centre, La Spezia, Italy, 1987.
- [12] I. T. Lu and L. B. Felsen, “Adiabatic transforms for spectral analysis and synthesis of weakly range-dependent shallow ocean Green’s functions,” *J. Acoust. Soc. Amer.*, vol. 81, pp. 897–911, 1987.
- [13] J. T. Goh and H. Schmidt, “Validity of spectral theories for weakly range-dependent ocean environments—Numerical results,” *J. Acoust. Soc. Amer.*, vol. 95, no. 2, pp. 727–732, 1994.
- [14] H. Schmidt, W. Seong, and J. T. Goh, “Spectral super-element approach to range-dependent ocean acoustic modeling,” *J. Acoust. Soc. Amer.*, vol. 98, no. 1, pp. 465–472, 1995.
- [15] J. T. Goh and H. Schmidt, “A hybrid coupled wavenumber integration approach to range-dependent seismo-acoustic modeling,” *J. Acoust. Soc. Amer.*, vol. 100, no. 3, pp. 1409–1420, 1996.
- [16] H. Schmidt, “Marching wavenumber-integration approach to range-dependent, two-way seismoacoustic propagation modeling,” *J. Acoust. Soc. Amer.*, vol. 97, no. 5, p. 3316 (A), 1995.
- [17] F. B. Jensen and C. M. Ferla, “Numerical solutions of range-dependent benchmark problems in ocean acoustics,” *J. Acoust. Soc. Amer.*, vol. 87, 1499–1510, 1990.
- [18] J. T. Goh, “Spectral super-element approach for wave propagation in range dependent elastic medium,” Ph.D. dissertation, Massachusetts Institute of Technology, Cambridge, June 1996.
- [19] S. A. Chin-Bing, D. B. King, J. A. Davis, and R. B. Evans, *Reverberation and Scattering Workshop—Proceedings of the Reverberation and Scattering Workshop*. Naval Research Laboratory, 1995.
- [20] P. Gerstoft and H. Schmidt, “A boundary element approach to seismo-acoustic facet reverberation,” *J. Acoust. Soc. Amer.*, vol. 89, pp. 1629–1642, 1991.
- [21] J. A. Davis, D. White, and R. C. Cavanaugh, presented at the NORDA Parabolic Equation Workshop, NORDA Tech. Note 143, 1982.
- [22] S. A. Chin-Bing, D. B. King, J. A. Davis, and R. B. Evans, *PE Workshop II—Proc. Second Parabolic Equation Workshop*, Naval Research Laboratory, 1993.



Joo Thiam Goh (M'96) was born in Singapore in 1961. He received the B.Eng. degree in electronics and control engineering from the University of Birmingham, U.K., in 1987 and the Ph.D. degree in acoustics from the Massachusetts Institute of Technology, Cambridge, in 1996.

From 1987 to 1991, he was an Engineer with the Defence Science Organisation (DSO) in Singapore, where he worked on real-time data acquisition systems and software for embedded computer systems. He is currently working as a Research Engineer at DSO. His primary research interest is in modeling the complex acoustic fields in ocean waveguides. Other interests include computational acoustics and distributed computing.

Dr. Goh is a member of the Acoustical Society of America.



Henrik Schmidt was born in Denmark in 1950. He received the M.S. degree in civil engineering and the Ph.D. degree in experimental mechanics from the Technical University of Denmark in 1974 and 1978, respectively.

Holding the position of Research Fellow from 1978 to 1980 at the Technical University of Denmark, and from 1980 to 1982 at Risoe National Laboratory, Denmark, he worked on numerical modeling of wave propagation and scattering phenomena in relation to nondestructive testing of structures. From 1982 to 1987, he was a Scientist and then Senior Scientist at SACLANT Undersea Research Centre, Italy, where he developed the SAFARI code for modeling seismo-acoustic propagation in ocean waveguides. In 1987, he joined the Massachusetts Institute of Technology, Cambridge, where he is currently Professor of Ocean Engineering and Associate Department Head in the Department of Ocean Engineering. His primary research interest is the interaction of underwater sound with seismic waves in the seabed and the Arctic ice cover. Other interests include computational acoustics and matched field processing and the use of acoustics in autonomous oceanographic sampling networks.

Prof. Schmidt is a fellow of the Acoustical Society of America and a member of the Society of Exploration Geophysicists.



Peter Gerstoft received the M.Sc. and the Ph.D. degrees from the Technical University of Denmark in 1983 and 1986, respectively, and the M.Sc. degree from the University of Western Ontario, Canada, in 1984.

From 1987 to 1992, he was employed at Ødegaard and Danneskiold-Samsøe in Denmark working on forward modeling for seismic exploration, and from 1989 to 1990, he was a Visiting Scientist at the Massachusetts Institute of Technology, Cambridge, and at Woods Hole Oceanographic Institute,

Woods Hole, MA. Since 1992, he has been a Senior Scientist at SACLANT Undersea Research Centre, La Spezia, Italy. His research interests include global optimization, modeling, and inversion of acoustic signals.

Dr. Gerstoft is a member of the Society of Exploration Geophysicists and the Acoustical Society of America.



Woojae Seong was born in Seoul, Korea, on January 6, 1960. He received the B.S. and M.S. degrees in naval architecture and ocean engineering from Seoul National University, Korea, in 1982 and 1984, respectively, and the Ph.D. degree in ocean engineering from the Massachusetts Institute of Technology, Cambridge, in 1991.

Presently, he is an Associate Professor in the Department of Ocean Engineering at Inha University, Inchon, Korea. His research interests are mainly in acoustic propagation modeling in realistic ocean environments.